Knowledge E
Engaging minds

Conference Paper

Induction Motor Fault Modeling Based on the Winding Function

Jorge Carrera, Rafael Franceschi, and Guadalupe Gonzalez

Universidad Tecnologica de Panama, Ciudad de Panama, Panama

Abstract

The deterioration in electrical equipment, is normal and its process begins as soon as the equipment is installed. Failure to inspect may cause faults. A failure in these devices can represent from thousands of dollars in losses of production to loss of lives, therfore, it is our responsibility as engineers to develop and apply techniques that ensure their optimal operation. There are several maintenance techniques, including condition monitoring which uses vibration and electrical data from motors/generators to diagnose faults. The objective of this work is to develop a computational model of an induction motor based on the winding function technique to model electrical and mechanical faults. This is the first step in order to proceed with a most comprehensive project about condition monitoring of induction machines under fault based on signal processing analysis.

Keywords: faults, induction machines, winding function

Corresponding Author:
Guadalupe Gonzalez
guadalupe.gonzalez@
utp.ac.pa

🔓 OPEN ACCESS

1. Introduction

According to the market research and consulting firm, Markets and Markets, the population of electric motors and drives is estimated to grow at a compound annual growth rate of 6.25%, from $10.26 billion in 2015 to $15.92 billion by 2022 (Mraz, 2017). These amounts are not surprising since electric motors are in virtually every aspect of our daily lives, from the operation of various industries including fuel and gas, power generation, marine, cement, mining, chemical and water treatment as well as in the transport sector, air conditioning systems in homes and commercial centers, in cell phone vibration systems, among others.

Consequently, electric motors and the systems they drive are the largest electrical end-use load, consuming between 43% and 46% of all global electricity, giving rise to about 6,040 Mt of CO_2 emissions, and costing the end-user about $565 billion per year on electricity bills. By 2030, its consumption is expected to rise to 13,360 TWh per year,

its CO_2 emissions to rise to 8570 Mt per year and will cost the end-user approximately $900 billion per year on electricity (Waide and Brunner, 2011).

Due to the rapid increment of the electric motors population it is necessary to continuously develop technology so that these equipment operate in an efficient and reliable manner. Failure to do so, could lead to major disasters. For instance, analyses from blackout events in the US show that a 30-minute power cut results in an average loss of US$15,709 for medium and large industrial clients, and nearly US$94,000 for an eight-hour interruption. Even short blackouts add up to an annual estimated economic loss of between US$104 and US$164 billion (Hodge, 2015).

2. Electric Motor Failures

The most common failures of electric motors in industry occur due to: surpassing the standard lifetime, wrong-rated power, voltage, and current, unstable supply voltage or current source, overload or unbalanced load, electrical stress from fast switching inverters or unstable ground, residual stress from manufacturing, mistakes during repairs and harsh application environment (dust, water leaks, environmental vibration, chemical contamination, high temperature).

Regarding induction motors, the principal type of failures are described in Figure 1. From these, 40% of the failures are due to bearings failures, 38% are stator related, 10% are due to the rotor and 12% to other failures (Toliyat, et al., 2013).
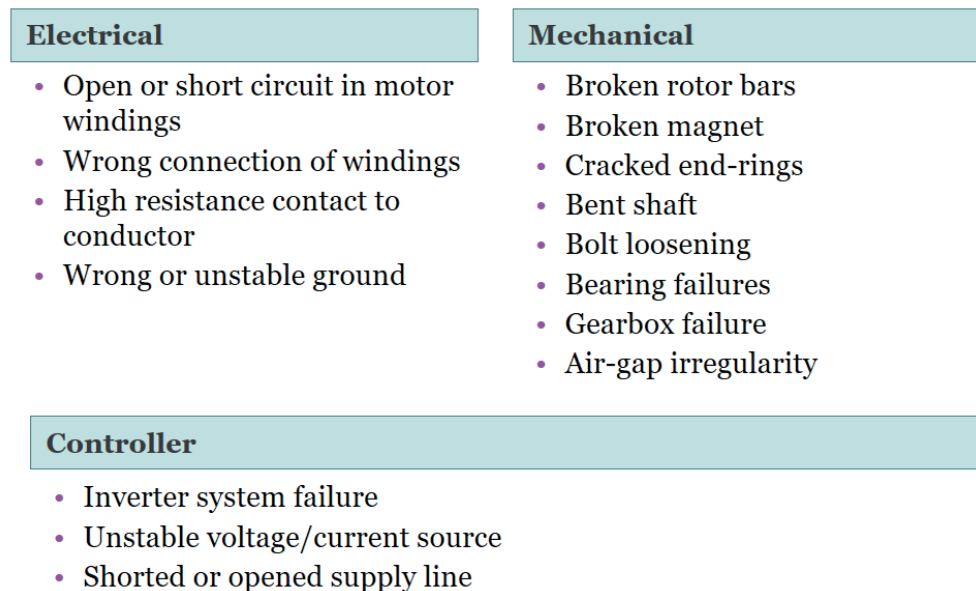
Electrical
- Open or short circuit in motor windings
- Wrong connection of windings
- High resistance contact to conductor
- Wrong or unstable ground

Mechanical
- Broken rotor bars
- Broken magnet
- Cracked end-rings
- Bent shaft
- Bolt loosening
- Bearing failures
- Gearbox failure
- Air-gap irregularity

Controller
- Inverter system failure
- Unstable voltage/current source
- Shorted or opened supply line

Figure 1: Principal types of failure in induction motors

It is important to point out that a motor under failure shows various abnormal symptoms, such as: mechanical vibrations, temperature increase, irregular air-gap torque, instantaneous output power variations, acoustic noise, line voltage change, line current changes and speed variations. All these abnormal symptoms leave specific patterns depending on the type and severity of the fault; for example, a particular frequency, amplitude, duration, variance, degree and phase (Toliyat, et al., 2013).

Some techniques adopted by the industry to diagnose and model faults are the following:

- Signal-based fault diagnosis

  – Mechanical vibration analysis, Shock pulse monitoring, Temperature measurement, Acoustic noise analysis, Electromagnetic field monitoring through inserted coil, Instantaneous output power variation analysis, Infrared analysis, Gas analysis, Oil analysis, Radio-frequency (RF) emission monitoring, Partial discharge measurement, Motor current signature analysis (MCSA), Statistical analysis of relevant signals

- Model-based fault diagnosis

  – Neural network, Fuzzy logic analysis, Genetic algorithm, Artificial intelligence, Finite-element (FE) magnetic circuit equivalents, Linear-circuit-theory-based mathematical models

- Machine-theory-based fault analysis

  – Winding function approach (WFA), Modified winding function approach (MWFA), Magnetic equivalent circuit (MEC), Simulation-based fault analysis, Finite-element analysis (FEA) and Time-step coupled finite element state space analysis (TSCFE-SS).

Comprehensive algorithms based on the aforementioned techniques are constantly under research, seeking that defects and their severity are reliably identified. For instance, there are commercial solutions that uses vibration and electrical measurements in combination, analyzing the data with a single instrument and software platform. This integrated approach avoids false data, accuracy problems and other issues that affect conventional methods based on separate analysis of vibration and electrical data.

3. Winding Function Method

The model of an induction motor developed in this work is based on the winding function method. This approach characterizes the machine in terms of coupled magnetic circuits rather than magnetic fields (Lipo, 2008). Usually, the way to analyze electric machines is to obtain the electromagnetic field distribution of the machine, which requires loads of computer resources and time. On the other hand, describing electric machines as group coupled magnetic circuits, usually inductance and resistance, provides a computational effective way of obtaining their operating characteristics since the winding structure dictates the magnetomotive force inside a machine and the air-gap the bulk of the permeance; flux, flux linkage, and hence, flux linkage per ampere turn or inductance can be easily computed using this method. Even effects such as saturation, slots, skewing and inclined rotor eccentricity can be included (Toliyat, et al., 2013).

Following Ibrahim et al. (2010), the mutual inductance between any two circuits can be calculated from:

$$L_{ij} = (\mu_0 Lr/g) \int_0^{2\pi} N_i(\theta_r, \Phi) N_j(\theta_r, \Phi) d\Phi \qquad (1)$$

where, Φ is a particular point along the air gap, and $N_i(\theta r, \Phi)$, $N_j(\theta r, \Phi)$ are winding function of circuit i and j and they are defined as the magneto motive force (MMF) distribution along the air gap for a unit current flowing in the winding.

For a sinusoidal distributed stator windings, the winding function for each phase is:

$$N_a(\theta_r, \Phi) = (N_s/2P) \cos(P\Phi)$$

$$N_b(\theta_r, \Phi) = (N_s/2P) \cos(P\Phi - (2\pi/3)) \qquad (2)$$

$$N_c(\theta_r, \Phi) = (N_s/2P) \cos(P\Phi + (2\pi/3))$$

where, $N_s = (4/\pi) N K_d K_p K_s$ = effective number of turns of winding, $N = p N_{tsp} N_{spp}$ = actual number of turns of windings, K_d, K_p and K_s are distribution, pitch, and skew factors, p is number of pole pairs, N_{tsp} is the number of turns per slot per phase, and N_{spp} is the number of slots per pole per phase.

For the rotor, the winding function of each rotor loops can be written as:

$$N_k(\theta_r, \Phi) = \begin{cases} -(\alpha_r/2\pi), & 0 < \Phi < \theta_k \\ 1 - (\alpha_r/2\pi), & \theta_k < \Phi < \theta_{k+1} \\ -(\alpha_r/2\pi), & \theta_{k+1} < \Phi < \theta_k \end{cases} \qquad (3)$$

where, $\alpha_r = (2\pi/n)$ = angle between any two adjacent bars,

$\theta_k = \theta_r + (k-1)\theta_r$ = bar k angular position.

4. Induction Motor Modeling

To develop our model, we followed Ibrahim et al. (2010) as they presented a detailed and simple way to achieve a model of a motor under stable conditions and under fault. Similarly, we defined the stator phase voltages (V_a, V_b, V_c) base on the stator phase currents (I_a, I_b, I_c), the stator phase self-inductances (L_a, L_b, L_c), the stator phase to phase mutual inductances (L_{ab}, L_{bc}, L_{ca}), the stator leakage inductance (L_{ls}), the rotor loops currents (I_{rn}), the end ring current (I_e) and each stator phase to rotor loop mutual inductances ($L_{a1},...,L_{an}$, $L_{b1},...,L_{bn}$, $L_{c1},...,L_{cn}$).

$$V_a = R_s I_a + (L_a + L_{Is})dI_a/dt + L_{ab}dI_b/dt + L_{ac}dI_c/dt$$

$$+d/dt(L_{a1}I_{r1} + L_{a2}I_{r2} + \cdots + L_{an}I_{rn} + L_{ae}I_e)$$

$$V_b = R_s I_b + (L_b + L_{Is})dI_b/dt + L_{ba}dI_a/dt + L_{bc}dI_c/dt$$

$$+d/dt(L_{b1}I_{r1} + L_{b2}I_{r2} + \cdots + L_{bn}I_{rn} + L_{be}I_e)$$

$$V_c = R_s I_c + (L_c + L_{Is})dI_c/dt + L_{ca}dI_a/dt + L_{cb}dI_b/dt$$

$$+d/dt(L_{c1}I_{r1} + L_{c2}I_{r2} + \cdots + L_{cn}I_{rn} + L_{ce}I_e)$$

$$(4)$$

The voltage equation for any rotor loop k is written based on the rotor bar resistance and inductance (R_b, L_b), end ring segment resistance and inductance (R_e, L_e), rotor loop self-inductance (L_{kk}), rotor loop mutual inductances ($L_{k1},...,L_{kn}$) and the rotor loop k to the stator windings mutual inductances (L_{ak}, L_{bk}, L_{ck}) :

$$0 = 2(R_b + R_e)I_{rk} - Rb(I_{r(k-1)} + I_{r(k+1)}) - R_e I_e$$

$$+2(L_b + L_e)dI_{rk}/dt - L_b(dI_{r(k-1)}/dt + dI_{r(k+1)}/dt)$$

$$+(L_{k1}dI_{r1}/dt + L_{k2}dI_{r2}/dt + \cdots + L_{kk}dI_{rk}/dt + \cdots + L_{kn}dI_{rn}/dt)$$

$$-L_e dI_e/dt + d/dt(L_{ak}I_a + L_{bk}I_b + L_{ck}I_c)$$

$$(5)$$

The end ring equation can be written as

$$0 = nR_e I_e - R_e(I_{r1} + I_{r2} + \cdots + I_{rn}) + nL_e dI_e/dt - L_e(dI_{r1}/dt + dI_{r2}/dt + \cdots + dI_{rn}/dt) \quad (6)$$

Furthermore, the electromagnetic torque equation can be written in terms of the electrical values and the rotor angular position as

$$T_{\text{em}} = I_a \left(\sum_{k=1}^{n} I_{rk} dL_{ak}/d\theta_r \right) + I_b \left(\sum_{k=1}^{n} I_{rk} dL_{bk}/d\theta_r \right) + I_c \left(\sum_{k=1}^{n} I_{rk} dL_{ck}/d\theta_r \right) \quad (7)$$

And finally, the rotor mechanical equation is given by the rotor inertia (J), the rotor angular speed (Ω_r), the friction coefficient (F) and the load torque (T_L)

$$T_{\text{em}} = Jd\Omega_r/dt + F\Omega_r + T_L \quad (8)$$

TABLE I
INDUCTION MOTOR PARAMETERS

INPUT SUPPLY PARAMETERS	
Input Supply Phase Voltage	220 Volt
Input Supply Frequency	50 Hz
STATOR PARAMETERS	
Effective Number of Stator winding turns: N_s	156 turn
Stator windings Ohmic resistance: R_s	1.5 Ω
Stator windings Leakage inductance: L_{ls}	7 mH
Number of pole pairs: p	1
ROTOR PARAMETERS	
Number of rotor bars: n	28
Rotor bar resistance: R_b	96.940036 $\mu\Omega$
End ring segment resistance: R_e	5 $\mu\Omega$
Rotor bar self inductance: L_b	0.28 μH
End ring segment self inductance: L_e	0.036 μH
AIR GAP PARAMETERS	
Air gap average radius: r	70 mm
Air gap length: g	0.28 mm
Rotor effective length: L	120 mm
MECHANICAL PARAMETERS	
Inertia: J	0.002N.sec^2
Friction coefficient: F	0.001N.sec

5. Simulation and Results

The model was done in MatLab and for the same 4kW induction motor with the parameters given in Table I by Ibrahim et al. (2010), we obtained the same results for a motor under healthy conditions and for one under rotor faults.

• Under healthy condition, the motor is simulated at no load for 0.5 seconds and then the motor is loaded with a load of 10 Nm. Figure 2 shows the speed and
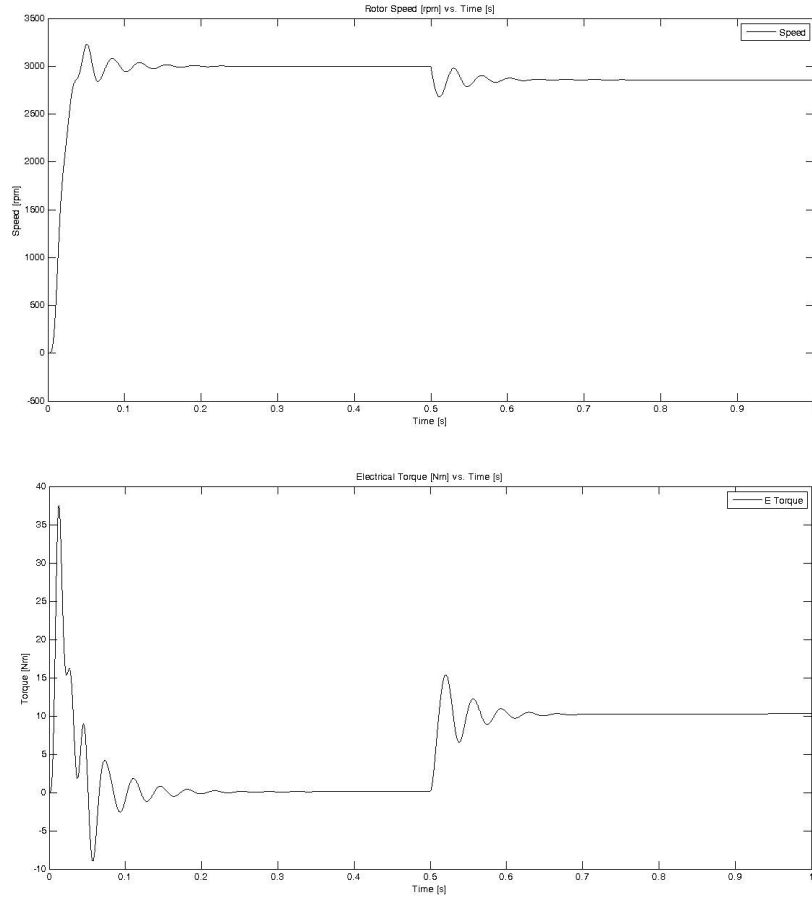
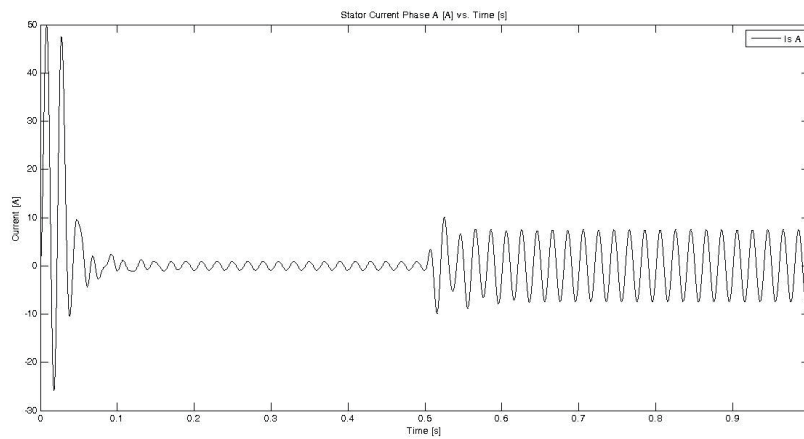**Figure** 2: Rotor speed and electrical torque

Figure 3: Phase A current

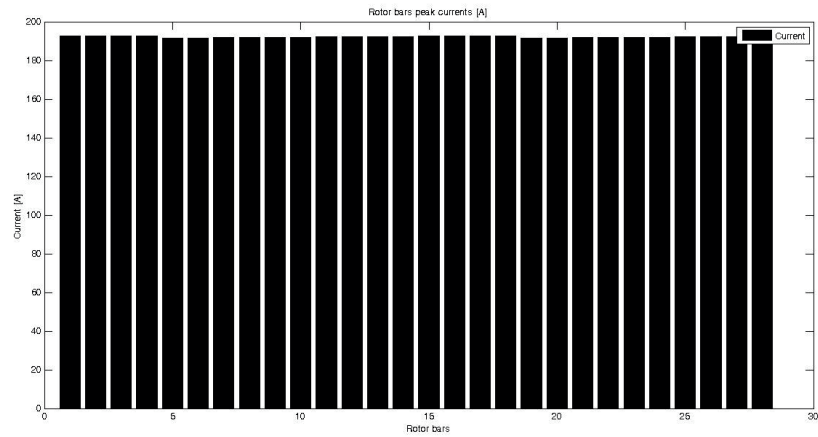torque, Figure 3 shows the phase A current and Figure 4 shows the rotor bar current distribution.

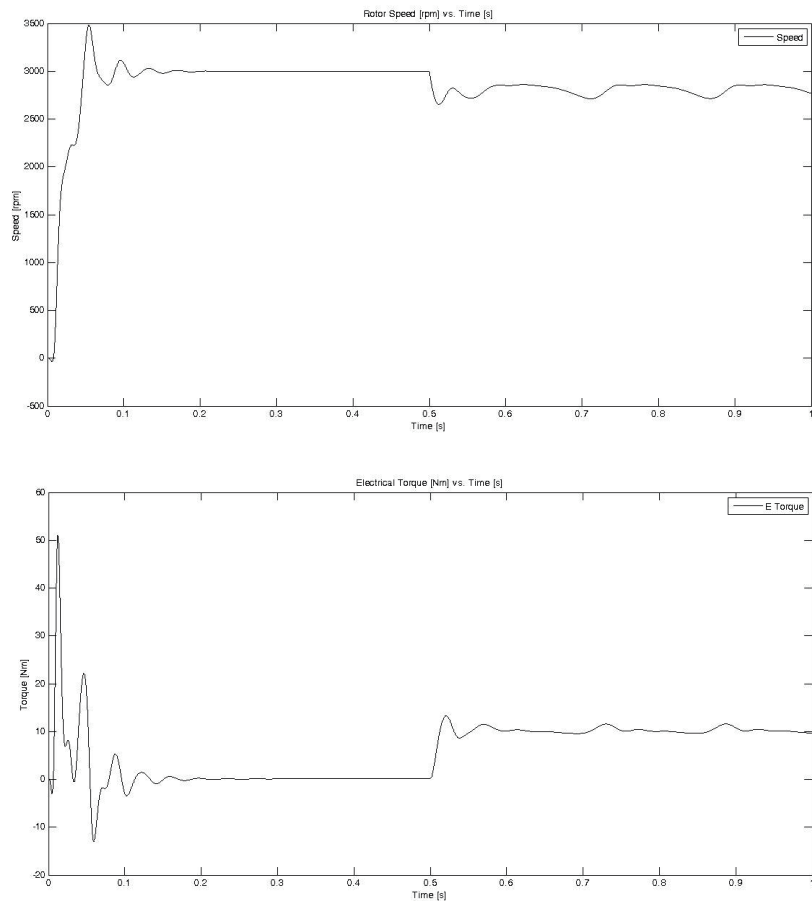**Figure** 4: Rotor bars current distribution

Figure 5: Rotor speed and electrical torque under fault

- Under fault, the motor is simulated with one broken bar and one broken end ring segment. Figure 5 shows the speed and torque, Figure 6 shows the phase A current and Figure 7 shows the rotor bar current distribution. It is important to point out that broken rotor bar faults can be simulated by increasing bar
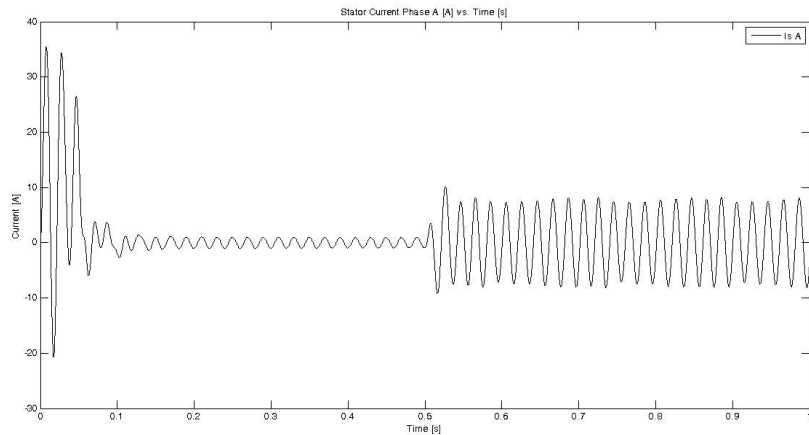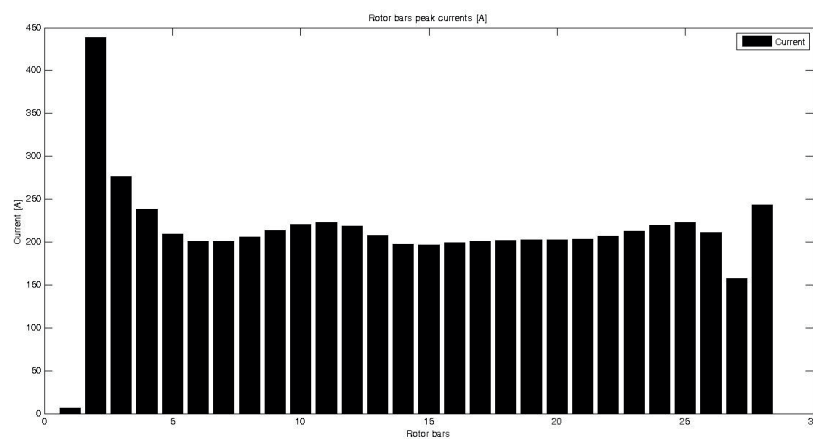
Figure 6: Phase A current under fault

Figure 7: Rotor bar distribution under fault

resistance. According to Ibrahim et. al., the more the resistance is increased the more severity is added to the fault. It is enough to increase bar resistance to 100 time of its original resistance to represent complete open rotor bar.

6. Conclusions

The objective of this first stage of the project was achieved. We were able to replicate the results of the model of the induction motor based on the winding function presented by Ibrahim et. al. both under healthy conditions and under various fault conditions.

Now that we are sure that we have a functional model we will be able to proceed with the next stage that is validate the model with experimentation, perform the

upgrades needed and proceed to pair the model with signal processing analysis to develop strategies for condition monitoring.

References

[1] Hodge, N. (2015), "Energy risks – the dangers of power cuts and blackouts", *INSIGHTS Special topic – Emerging risks*, Allianz Global Corporate & Specialty, AGCS ALLIANZ, pp. 28-33. Available online: http://www.agcs.allianz.com/insights/expert-risk-articles/energy-risks/

[2] Ibrahim, A.K., Marei, M.I., El-Gohay H.S., Shehata, S.A., "Modeling of Induction Motor Based on Winding Function Theory to Study Motor under Stator/Rotor Internal Faults", Proceedings of the 14th International Middle East Power Systems Conference (MEPCON'10), Cairo University, Egypt, December 19-21, 2010, Paper ID 215.

[3] Lipo, T. A. (2008), *Analysis of Synchronous Machines*, WisPERC Administrator, University of Wisconsin-Madison

[4] Mraz, S. (2017). "The Market Outlook for Motors and Drives through 2022". *Machines Design*, Published on February 16, 2017. Available online: http://www.machinedesign.com/motorsdrives/market-outlook-motors-and-drives-through-2022.

[5] Toliyat. H., Nandi, S., Choi S., and Meshgin-Kelk, H. *Electric Machines: modeling, conditioning monitoring, and fault diagnosis*, CRC Press, 2013

[6] Waide, P., and Brunner, C.U. (2011). "Energy-efficiency policy opportunities for electric motor-driven systems", *International Energy Agency*, France. pp.11. ISSN: 2079-2581. Available online: www.iea.org/Textbase/npsum/ee_for_electricsystemssum.pdf

Authorization and Disclaimer

Authors authorize ESTEC to publish the paper in the conference proceedings. Neither ESTEC nor the editors are responsible either for the content or for the implications of what is expressed in the paper.